Article

Not peer-reviewed version

Research on the Rheological Property and Modification Mechanism of MWCNTs-OH/SBS Modified Asphalt Binder

Manman Su * , Qi Ding , Zuohong He , Xuling Huang , Leilei He , Enlong Zhao

Posted Date: 24 April 2025

doi: 10.20944/preprints202504.2078.v1

Keywords: Hydroxylated multiwalled carbon nanotubes; composite modified asphalt; rheological properties; modification mechanism; X-ray diffraction

Article

Research on the Rheological Property and Modification Mechanism of MWCNTs-OH/SBS Modified Asphalt Binder

Manman Su [1,*], Qi Ding [1], Zuohong He [2], Xuling Huang [1], Leilei He [1] and Enlong Zhao [1]

[1] School of Civil Engineering, Yantai University, Yantai Shandong 264005, China; 3485308452@qq.com; huangning.139@163.com; 916160320@qq.com; 2750273083@qq.com

[2] China Railway 23rd Bureau Group Co., Ltd, Linyi Shandong 276000, China; 674208193@163.com

* Correspondence: suman0725@ytu.edu.cn

Abstract: The objective of this study is to explore the high temperature rheological properties of hydroxylated multiwalled carbon nanotubes (MWCNTs-OH) and styrene-butadiene-styrene (SBS) composite modified asphalt, and reveal the modification mechanism. Three types of modified asphalts including SBS modified asphalt, carbon nanotube modified asphalt and MWCNTs/SBS composite modified asphalt were prepared with high-speed shearing apparatus and machine mixer. The basic physical properties, dynamic shear rheometer (DSR) test, and multiple stress creep recovery(MSCR) test were conducted to modified asphalt and base asphalt to evaluate the influence of MWCNTs-OH and SBS on the high temperature properties of asphalt. X-Ray diffraction (XRD) and Raman spectroscopy were involved to study the modification mechanism. From the DSR tests and MSCR tests, it can be seen that the complex modulus (G*), phase angle (δ), rutting factor (G*/sin δ), creep recovery rate (R) and non-recoverable compliance (J_{nr}) of composited modified asphalt are better than the other three types of asphalts, which indicated that the synergistic effect of SBS and carbon nanotubes was beneficial to the improvement of the high-temperature performance of asphalt pavements. According to XRD test results, the addition of SBS/MWCNTs-OH reduced the crystallinity of the crystalline phase components in the asphalt mixture. MWCNTs-OH endowed SBS modified asphalt with better crystallinity and a higher content of the crystalline phase. Thus, the deformation resistance of SBS modified asphalt was improved. Raman spectroscopy showed that the intensity of the D and G peaks of the composite modified asphalt was enhanced and the chemical bond vibration was altered, which suggested that a strong chemical interaction occurred between modifier and asphalt and led to the potential improvement in mechanical properties of asphalt.

Keywords: Hydroxylated multiwalled carbon nanotubes; composite modified asphalt; rheological properties; modification mechanism; X-ray diffraction

---

1. Introduction

In recent years, the construction of expressways in China has been developing rapidly. The continuously increasing traffic flow and harsh environmental conditions had led to serious rutting and cracking diseases on the asphalt pavement. So, to retard the distress and improve the performance of asphalt pavement, the modified asphalt is widely studied and used during the construction of asphalt pavement[1]. At present, the performance of asphalt has been significantly enhanced by adding modifiers such as polymers, rubbers, and resins into base asphalt[2-6]. However, with the continuous expansion of the scale of expressway construction, many traditional modifiers are unable to meet the high performance and high standard requirements of asphalt pavement. With the continuous exploration and development of materials research, nanomaterials such as nanofibers, nanoparticles, nanoclays, and carbon nanotubes have opened up a new path for improving the asphalt performance[7-9]. Compared with other nanomaterials, carbon nanotubes have an extremely

Preprints.org (www.preprints.org) | NOT PEER-REVIEWED | Posted: 24 April 2025 doi:10.20944/preprints202504.2078.v1

high aspect ratio and outstanding mechanical strength which make it act as "reinforcing bars" during the modification process, and effectively restricting the movement of asphalt molecules.

Mansourkhaki et al [10] found that asphalt mixtures with carbon nanotubes exhibited higher ability to resist the low-temperature cracking compared to unmodified asphalt mixtures. Xue et al [11] discovered that carbon nanotubes could significantly improve the microwave thermal conductivity of asphalt, and the higher the dosage, the better the thermal conductivity. Santagata et al [12] concluded that the addition of carbon nanotubes reduces the sensitivity of asphalt to oxidative aging, which was beneficial for extending its service life. Amin et al [13] confirmed that both the fatigue cracking resistance and low-temperature cracking resistance of asphalt deteriorate as the content of carbon nanotubes increases. Gong et al [14] reported that the addition of CNTs improved the high-temperature performance and aging resistance of asphalt while decreasing its low-temperature performance. Goli A et al [15] pointed out that the addition of carbon nanotubes reduced the penetration index, and temperature sensitivity of asphalt, and effectively improved the physical properties, rheological properties and stability of the asphalt binder. Shah et al [16] based on basic physical tests and rheological tests, found that the addition of multi-walled carbon nanotubes improves the aging resistance of the asphalt binder, and the low temperature performance of MWCNTs was not encouraging. Latifi et al [17] evaluated the properties of carbon nanotubes asphalt binders through microscopic and macroscopic tests. The results showed that the modification with carbon nanotubes could enhance the stiffness of asphalt mixtures, and thus improve the rutting resistance. The modification with carbon nanotubes also improved the fatigue resistance of hot mix asphalt (HMA) specimens, especially under low temperature conditions.

Mamun et al [18] demonstrated that after adding carbon nanotubes, the moisture damage of single-walled carbon nanotube/SBS composite modified asphalt was reduced. In addition, Zhu et al [19] revealed that carbon nanotubes could improve the high and low temperature performance of SBS modified asphalt. Through microscopic tests, Fu et al [20] found that carbon nanotubes restricted the movement between SBS particles and asphalt molecules, and resulted in a more uniform dispersion of SBS in asphalt and improved its compatibility and storage stability. Sun et al [21] confirmed that after adding CNTs, the temperature sensitivity of SBS modified asphalt was improved, and its high-temperature performance and anti-aging property were enhanced, while the low-temperature performance was less affected. Obukhova et al [22] pointed out that single-walled carbon nanotubes increased the durability parameters of the binder by 150%, and improved the relaxation performance at low temperatures, and enhanced the resistance to fatigue damage. Tang et al [23] studied the influence of carbon nanotubes on the high-temperature rheological properties and chemical properties of SBS modified asphalt through the molecular dynamics simulation, DSR, BBR, and FTIR tests. The addition of carbon nanotubes can improve the rheological properties, temperature sensitivity, and high-temperature rutting resistance of SBS modified asphalt. Chen et al [24] found that CNT/SBS composite modified asphalt had an outstanding storage stability and workability, and the DSR results indicated that composite modified asphalt exhibited excellent resistance to high temperature, aging, and deformation.

Nowadays, many studies have been carried out on the modification mechanism of modified asphalt. Wang et al [25] conducted Raman spectroscopy, XRD and Fourier transform infrared spectroscopy techniques, and concluded that CNT/SBS modifier had high crystallinity, high degree of graphitization and few defects, and chemical reaction didn't occur between CNT and asphalt. Yu et al [26] reported that carbon nanotubes made the distribution of aromatics and saturates more uniform, and alleviated the competition between SBS and asphaltenes. Zhang et al [27] found that MWCNTs enhanced the cross-linking between the SBS modifier and the asphalt binder, and improved the distribution of the polar components in the asphalt binder by molecular dynamics and AFM testing methods. Wang et al [28] pointed out that the C=C bonds of carbon nanotubes could interact with the alkanes and aromatic hydrocarbons in asphalt, and the synergistic effect between the carbon nanotubes and SBS due to the π-π conjugation of the benzene rings enabled SBS to adsorb and wind around the carbon nanotubes, thus improved the mechanical properties. Shu et al [29] revealed that saturates and aromatics of asphalt penetrated into the network structure of SBS in the MWCNT/SBS modified asphalt and formed a more stable network structure, and brought asphalt a

Preprints.org (www.preprints.org) | NOT PEER-REVIEWED | Posted: 24 April 2025 doi:10.20944/preprints202504.2078.v1

significant improvement of high-temperature and low-temperature properties. Nie et al [30] noticed that MWCNTs enhanced the intermolecular interactions by increasing the van der Waals energy of the MWCNTs/SBS modified asphalt, and resulted stability of the system against external loads and improved the mechanical properties of asphalt. Although plenty of researches have been conducted to characterize morphology and dispersion of SBS and MWCNTs in asphalt binder, the reason of the improvement of SBS and MWCNTs on properties of base asphalt haven't been explored thoroughly and comprehensively. Moreover, the X-ray diffraction and Raman spectroscopy method is used to reveal the modification mechanism of SBS/MWCNTs composite modified asphalt is almost blank.

Therefore, in this study, the basic physical properties experiments including penetration, softening point, ductility and viscosity, as well as rheological property tests such as DSR and MSCR were carried out to base asphalt, SBS modified asphalt, MWCNTS modified asphalt and composite modified asphalt. The influence of SBS and MWCNTs on the viscoelastic behavior as well as the resistance to rutting and stability of base asphalt binder was analyzed and evaluated. The modification mechanism of SBS/MWCNTs composite modified asphalt was investigated by XRD and Raman spectroscopy tests.

2. Materials and Experimental Methods

2.1. Materials

(1) Asphalt

In this study, the PG64-16 base asphalt produced by China Petrochemical Corporation was used, and its basic property indices were tested in accordance with the Chinese specification-"Standard Test Methods of Bitumen and Bituminous Mixtures for Highway Engineering ", and the results are shown in Table 1.

Table 1. Basic properties of base asphalt binder.

Properties	values	Test Standard
Penetration (25°C, 100g, 5s, 0.1mm)	72	
Softening point (5°C, °C)	46.6	
60°C dynamic viscosity (Pa·s)	Cm220	Specification of China (JTG E20-2011)
Ductility (10°C, 5 cm/min, cm)	56	
Flash point (°C)	>300	
Density (15°C, g/cm^3)	1.037	

(2) SBS Modifier

In this research, the linear SBS modifier produced by Dongguan Jinheng Company was adopted. The SBS particles (see Fig. 1) with a diameter of 3mm was used as modifier in this study. The SBS with a linear structure, and the ratio of styrene and butadiene was 31:69, and its basic properties were presented in Table 2.

Table 2. Properties of linear SBS modifier.

Properties	Values
S/B	31/69
Tensile strength (MPa)	32
Breaking elongation (%)	880
Hardness (10s)	72
Specific gravity	0.94

 doi:10.20944/preprints202504.2078.v1

Figure 1. SBS modifier.

(3) Multiwalled Carbon Nanotube

The hydroxylated multiwalled carbon nanotubes (MWCNTs-OH) produced by JiaCai Technology were utilized. The MWCNTs were in the state of black powder, and with a length less than 10μm, and a diameter of 40-60nm, and a specific surface area was 60-100m²/g. The specific property indices of MWCNTs were described in Table 3, and their macroscopic and microscopic morphologies were given in Fig. 2.

Table 3. Properties of MWCNTs.

Parameters	Values
Purity (%)	>98
Diameter (nm)	40-60
Length (μm)	<10
Specific surface area (m²/g)	60-100
Production method	Chemical vapor deposition (CVD)

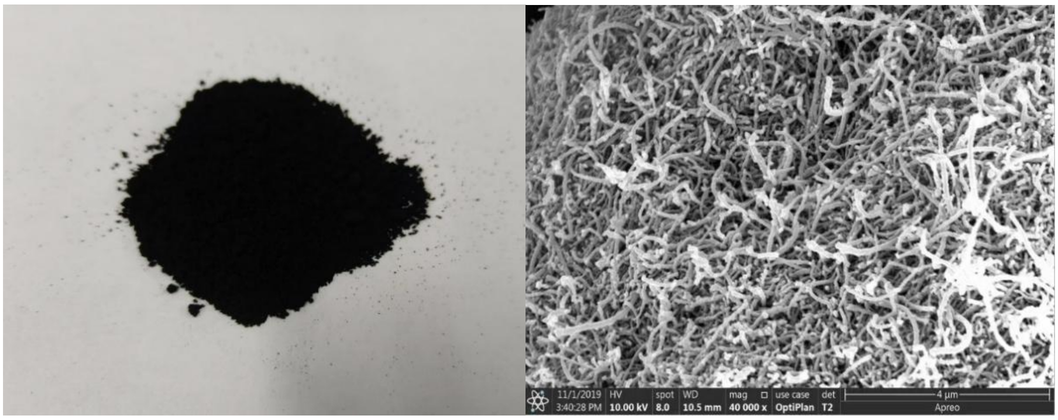

(a) (b)

Figure 2. The morphology of multiwalled carbon nanotubes (a) macroscopic and (b) microscopic.

2.2. Preparation of Modified Asphalt

Due to the high surface energy and easy agglomeration of carbon nanotubes, it is difficult to disperse MWCNTs modifier in process of preparing MWCNTs/SBS modified asphalt. In this research, high-speed shearing apparatus and machine mixer were used to prepare MWCNTs/SBS composite modified asphalt. The specific preparation steps are shown in Fig. 3: Firstly, heated the base asphalt to 160°C to make it turn to the flow state, and then SBS modifier was added into base asphalt slowly. Then, to achieve a better dispersion of SBS in base asphalt, the SBS and asphalt blends were stirred for 15 minutes at the rotation speed of 400rpm by using a machine mixer, and then were sheared for 50 minutes at the rotation speed of 5000 rpm by high-speed shear apparatus. Then the multiwalled carbon nanotubes was added slowly and stirred at a low-speed of 400rpm, and then sheared the mixture at the speed of 5000 rpm for 40 minutes. The stirring and shearing process of mixture was carried out at a temperature of 170°C. Finally, curing in the oven at 170°C for 1 hour [31-33].

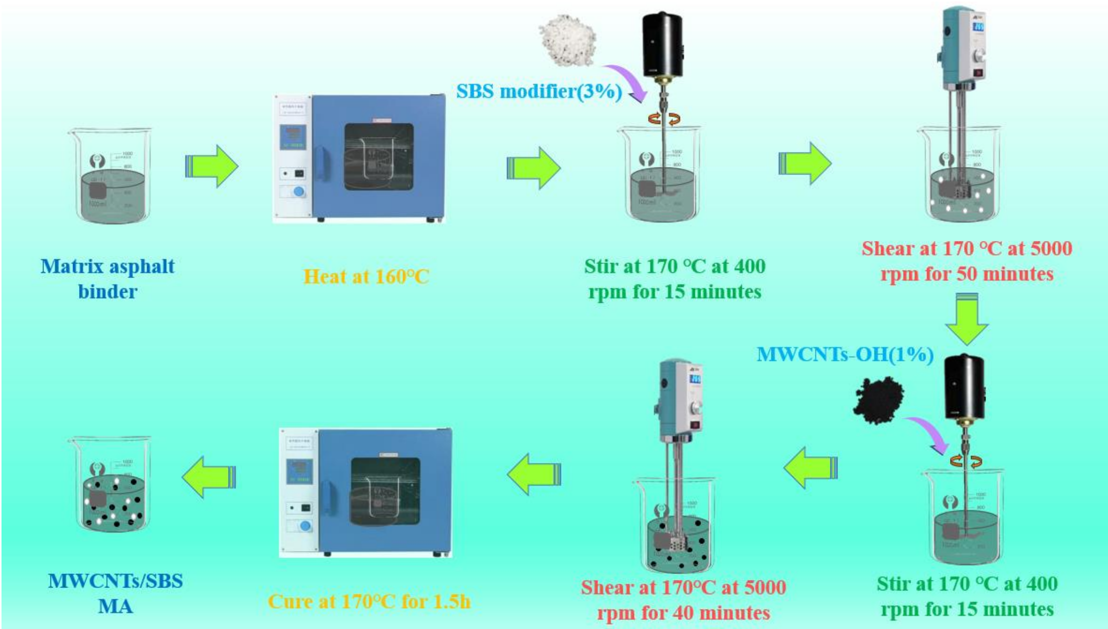

Figure 3. Preparation process of MWCNTs/SBS composite modified asphalt.

2.3. Experimental Method

(1) Basic physical property tests

The basic physical properties of base asphalt, SBS modified asphalt (SBS MA), MWCNTs modified asphalt (MWCNTs MA) and MWCNTs/SBS composite modified asphalt (MWCNTs/SBS MA) were evaluated through penetration, ductility, softening point tests and Brookfield rotational viscosity tests. The test temperatures for penetration, softening point, and ductility were set at 25°C, 5°C and 5°C, respectively. The viscosity test was carried out in the temperature range of 110-175°C. All the above-mentioned tests were carried out in accordance with the specification of China-"Standard Test Methods of Bitumen and Bituminous Mixtures for Highway Engineering"- (JTG E-20-2011).

(2) Dynamic shear rheological test

In this research, DSR tests were conducted to base asphalt and modified asphalt by following AASHTO T315-19. In this test, a 25-mm parallel plate with a plate spacing of 1 mm was used. The frequency sweep range was performed from 0.1 to 100 rad/s, and at a constant sweep frequency of 10 rad/s the temperature sweep test was carried out at the temperature of 50°C, 58°C, 66°C, 74°Cand 82°C. The high-temperature rheological properties of asphalt were analyzed through the complex modulus (G*), phase angle (δ) and rutting factor (G*/sin δ).

(3) Multiple stress creep test

The MSCR test was closely related to the high-temperature performance of asphalt. The creep recovery rate (R) and non-recoverable compliance (J_{nr}) of asphalt binder were measured by MSCR according to ASTM D7405-15. The creep stress levels were selected at 0.1 kPa and 3.2 kPa, which could simulate the deformation of asphalt under normal traffic loads and heavy traffic loads. Ten cycles were carried out at each stress level, with each cycle lasting 10 s (loading for 1 s and unloading for 9 s) and repeated for ten cycles [34].

(4) Microscopic tests

In this research, an X-ray diffractometer of the German Bruker-D8Advance model was used to conduct XRD tests on the four types of asphalt. The asphalt samples were in the form of 2×2 cm thin

 doi:10.20944/preprints202504.2078.v1

films. The test required the film thickness was about 1 mm. A Co-target was used for testing, and the asphalt was scanned at a rate of 8°/min in the conventional mode, with the test angle range of 10-90°. In the Raman test, a 633-nm excitation light source was selected, the scanning range was 50-4000, and the sample size was 2×2 cm. By analyzing the characteristic peaks of the crystal structure in the XRD spectrum and the changes in the peak position and intensity of the Raman spectrum, the differences in the microscopic structure of different types of asphalts were deeply explored.

3. Results and Analysis

It has been determined through previous research that when the dosage of SBS modified asphalt was 3% and that of carbon nanotube modified asphalt was 1%, the high-temperature rutting resistance and deformation resistance of asphalt can be effectively enhanced. In this study, the SBS modifier (3%) and MWCNTs modifier (1%) were applied to explore the effect on the mechanical properties of composite modified asphalt.

3.1. Basic Physical Properties

3.1.1. Penetration, Softening Point and Ductility

The results of penetration, softening point and ductility of base asphalt and modified asphalts were described in Fig. 4. As can be witnessed, the penetration of base asphalt, SBS modified asphalt, carbon nanotube modified asphalt and composite modified asphalt was 7.1mm, 7.67mm, 6.6mm and 6.93mm, respectively. Compared to other asphalt, SBS increased the penetration value greatly for its characteristic of thermoplastic rubber, which indicated that SBS improved the toughness of the asphalt. While, when the MWCNTs-OH was added to base asphalt, the surface active groups of MWCNTs-OH adsorbed with the asphalt and restricted the movement of asphalt molecular, which resulted in a decrease in penetration.

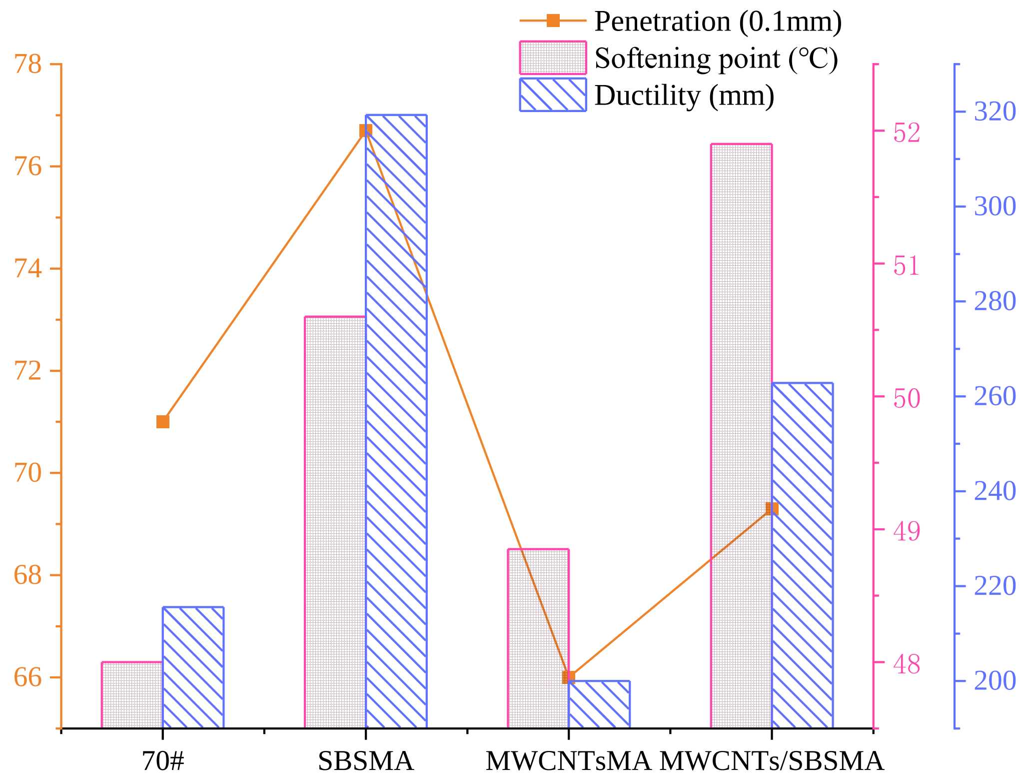

Figure 4. Results of penetration, softening point and ductility.

The results showed that compared with base asphalt the softening points of SBS modified asphalt, MWCNTs modified asphalt and composite modified asphalt increased by 2.6 °C, 0.9°C and 3.9°C, respectively. This implied that that the MWCNTs and SBS modifiers could significantly improve the high temperature property of asphalt, and the MWCNTs had a positive effect on the stability of SBS modified asphalt and brought MWCNTs/SBS composite modified asphalt better anti-deformation ability. The changes can be explained that the outstanding surface area of multiwalled carbon nanotubes led to a strong interface with asphalt and SBS, and resulted in a favorable network structure for asphalt.

It also can be seen that among the four types of asphalts, the improvement effect of SBS on ductility was the most obvious, while the MWCNTs exhibited a negative effect on ductility of asphalt. That's because the aggregation of MWCNTs affected the uniformity of the modified asphalt, which caused the stress concentration in local areas. Compared with the base asphalt, the ductility of the MWCNTs/SBS composite modified asphalt increased from 215.6mm to 262.8mm, which indicated that MWCNTs/SBS modifier improved the anti-cracking performance at low temperature The reason may be that the adding of SBS alleviated the aggregation of MWCNTs in matrix asphalt and enhanced flexibility of asphalt.

3.1.2. Viscosity-Temperature Relationship

The Brookfield viscosity reflects the frictional resistance generated by the relative motion between two fluid layers in asphalt. The higher the viscosity, the better the high-temperature rutting performance of the asphalt. Fig. 5 showed the viscosity-temperature relationship of asphalt. From 110℃ to 175 ℃, the viscosity of different types of asphalts decreased with the increase in temperature. The addition of MWCNTs or SBS led to an increase in viscosity. Under the same SBS content (3%), the viscosity of MWCNTs/SBS composite modified asphalt was exceed than SBS modified asphalt. This is attributed to the strengthening effect of carbon nanotubes. Carbon nanotubes were uniformly dispersed in the asphalt to form a reinforcing skeleton, which increased the internal friction force, and hindered the flow of asphalt molecules. Compared with the SBS modified asphalt, the viscosity values of the composite modified asphalt at each temperature increased by 0.11 Pa·s, 0.15 Pa·s, 0.111 Pa·s, 0.153 Pa·s and 0.186 Pa·s, respectively. The results of the viscosity experiment indicated that adding carbon nanotubes to SBS modified asphalt can further reduce its fluidity, increase its viscosity, and enhance its high-temperature rutting resistance.

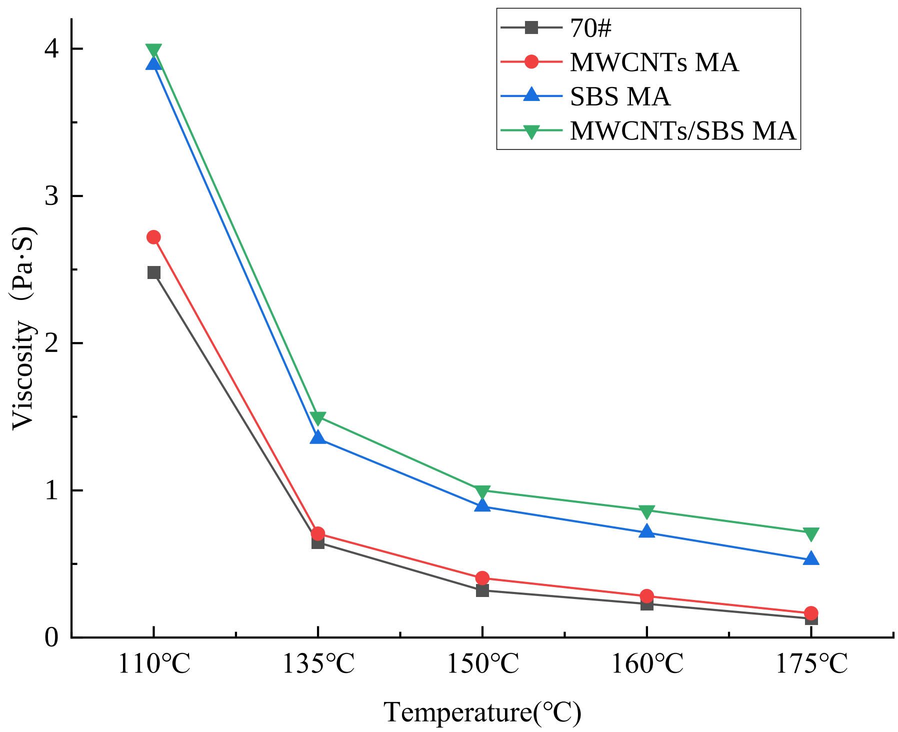

Figure 5. Curves of viscosity-temperature.

Preprints.org (www.preprints.org) | NOT PEER-REVIEWED | Posted: 24 April 2025 doi:10.20944/preprints202504.2078.v1

In addition, the optimal fitting equation was determined by comparing three common fitting equations for viscosity-temperature relationship [35-37]. The comparison of fitting equations is as follows:

$$\lg\boldsymbol{\eta} = n\text{-}m\times T \tag{1}$$

$$\lg\lg(\eta\times 10^3) = n\text{-}m\lg(T+273.13) \tag{2}$$

$$\boldsymbol{\eta}=AT^b \tag{3}$$

where η is the viscosity (Pa·s); T is the Celsius temperature (°C); n and m are fitting parameters; A and b are both regression constants.

Table 4. Fitting information of equation (1).

Equation	lg**η**=n-m×T			
Sample	Basic asphalt	CNTs MA	SBS MA	CNTs/SBS MA
Fitting equation	lg**η**=2.8511-0.0223×T	lg**η**=2.8068-0.0216×T	lg**η**=2.3405-0.0160×T	lg**η**=2.1751-0.0144×T
Reduced Chi-Sqr	0.00163	0.00451	0.02543	0.04427
R^2	0.9983	0.996	0.98674	0.97625

Table 5. Fitting information of equation (2).

Equation	lglg(**η**×10³)=n-mlg(T+273.13)			
Sample	Basic asphalt	CNTs MA	SBS MA	CNTs/SBS MA
Fitting equation	lglg(η×10³) = 2.6034 − 1.0136×lg(T + 273.13)	lglg(η×10³) = 2.4323 − 0.9282×lg(T + 273.13)	lglg(η×10³) = 1.7721 − 0.5975×lg(T + 273.13)	lglg(η×10³) = 1.5962 − 0.5112×lg(T + 273.13)
Reduced Chi-Sqr	2.54982E-5	1.38724E-5	1.14701E-5	4.0051E-5
R^2	0.99691	0.998	0.99601	0.98126

Table 6. Fitting information of equation (3).

Equation	**η**=A**θ**ᵇ			
Sample	Basic asphalt	CNTs MA	SBS MA	CNTs/SBS MA
Fitting equation	**η**=5.18126E13×$T^{-6.52504}$	**η**=2.05832E13×$T^{-6.30928}$	**η**=1.86322E10×$T^{-4.74324}$	**η**=2.29149E9×$T^{-4.29213}$
Reduced Chi-Sqr	1.27112E-4	0.00105	0.00892	0.01989
R^2	0.9999	0.9993	0.99651	0.992

The fitting information of the three fitting equations was displayed in Tables 4 to 6. The smaller the Reduced Chi-Sqr, the higher the fitting accuracy. The Reduced Chi-Sqr values of the three fitting equations were sorted as follows: equation(1) > equation(3) > equation(2). Therefore, the Saal equation was chosen to fit the viscosity-temperature curve. The fitting information was shown in Fig. 6. The slope of the linear equation represents the temperature sensitivity. It can be seen that the slope of the three modified asphalts were lower than that of the base asphalt, and the slope of MWCNTs/SBS composite modified asphalt was the lowest, indicating that adding SBS or MWCNTs to asphalt binder can improve the temperature sensitivity, and adding carbon nanotubes to SBS modified asphalt can effectively improve the workability of the asphalt pavement.

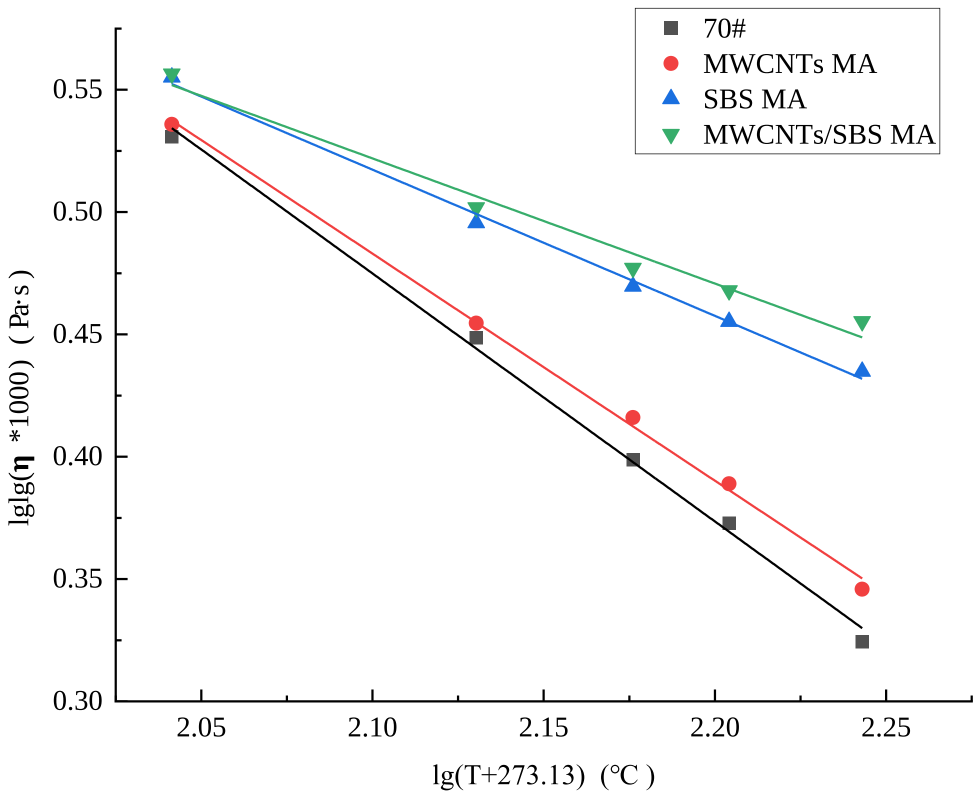

Figure 6. Asphalt viscosity-temperature curve.

3.2. Dynamic Shear Rheological Test

3.2.1. Frequency Sweeping

Frequency sweeping is a method for studying the rheological properties of asphalt. In order to evaluate the influence of additives on the viscoelastic properties of asphalt and understand the mechanical response of asphalt under different loading frequencies, taking the MWCNTs/SBS composite modified asphalt as an example, and the master curves were generated at a reference temperature of 50°C with the time-temperature equivalence principle [38]. The Williams-Landel-Ferry (WLF) non-linear equation was applied as the fitting equation for the shifting factor [39].The equation was given in Eq.(4). The shifting factor at each temperature was shown in Table 7.

$$\lg \boldsymbol{\phi}_T = -\frac{C1\cdot(T-T0)}{C2+(T-T0)} \tag{4}$$

where $\boldsymbol{\phi}_T$ is shifting factor; T is actual loading temperature; T_0 is Reference temperature ; C1 and C2 are fitting parameters of WLF non-linear equation.

Table 7. Information on shifting factors of different asphalts.

Sample	Shifting factor				
	50°C	58°C	66°C	74°C	82°C
Basic asphalt	0	-0.5094	-0.8384	-1.1629	-1.4070
SBS MA	0	-0.4414	-0.7891	-1.0005	-1.2087
MWCNTs MA	0	-0.5155	-0.9187	-1.1740	-1.3586
MWCNTs/SBS MA	0	-0.4609	-0.7362	-1.4089	-1.5084

Preprints.org (www.preprints.org) | NOT PEER-REVIEWED | Posted: 24 April 2025 doi:10.20944/preprints202504.2078.v1

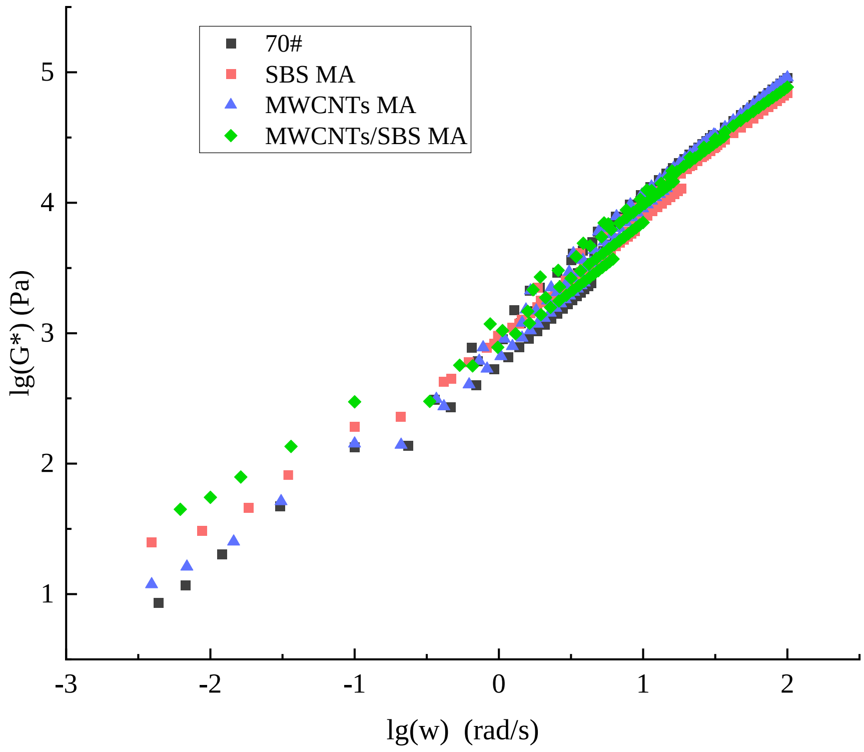

Figure 7. Master curve of complex modulus-frequency.

Fig. 7 displayed the master curve of complex modulus-frequency at temperatures of 50℃, 58℃, 64℃, 74℃ and 82℃. As shown in Fig. 7, the addition of 3%SBS or 1%MWCNTs modifiers increased the complex modulus in the overall range of loading frequency and in different temperatures. The higher the complex modulus, the greater the rutting resistance. Attributed to the complex interactions between carbon nanotubes and SBS, the MWCNTs/SBS composite modified asphalt demonstrated superior complex moduli compared with the SBS modified asphalt and the carbon nanotube modified asphalt, indicating that the addition of carbon nanotubes to SBS modified asphalt endows SBS modified asphalt with strong rutting resistance. With the increase of frequency, the complex modulus of asphalt showed an upward trend. It can be observed that the slope of the MWCNTs/SBS composite modified asphalt is smaller than that of the other three asphalts, which exhibited a better temperature sensitive performance.

3.2.2. Temperature Sweeping

As a typical viscoelastic material, asphalt displayed remarkable temperature dependence. The temperature sweeping test can systematically explore the viscoelastic response of asphalt within various temperature ranges. Fig. 8 illustrated the results of the temperature sweeping tests for base asphalt, SBS modified asphalt, carbon nanotube modified asphalt and MWCNTs/SBS composite modified asphalt with the temperature of 50, 58, 66, 74 and 82℃ at a sweeping frequency of 10 rad/s. The outcomes demonstrated that both the complex modulus and the phase angle of different types of asphalts displayed the same trend. With an increase in temperature, the complex shear modulus decreased, and the phase angle increased and then decreased. The possible reason was that the asphalt closed to the state of Newtonian fluid at high temperatures, and the phase difference between stress and strain were determined by its viscous characteristics. The phase angles values were sorted as follows: base asphalt > carbon nanotube modified asphalt > SBS modified asphalt > MWCNTs/SBS composite modified asphalt. In comparison with the base asphalt, the separate incorporation of MWCNTs and SBS significantly improved the complex shear modulus and phase angle of the asphalt. Compared with the SBS modified asphalt, the co-incorporation of MWCNTs and SBS into the asphalt contributed to a higher complex modulus and a lower phase angle. This is due to the fact that carbon nanotubes possess large specific surface area and high aspect ratio. After adding carbon

Preprints.org (www.preprints.org) | NOT PEER-REVIEWED | Posted: 24 April 2025 doi:10.20944/preprints202504.2078.v1

nanotubes to the SBS modified asphalt, the structure of the SBS modified asphalt became more compact, and thus, MWCNTs substantially enhanced the deformation recovery ability of the SBS modified asphalt. The SHRP specification defined the rutting factor to signify the resistance of asphalt materials to permanent deformation, which can characterize the high-temperature properties of asphalt. The greater the rutting factor, the superior the rutting resistance of the asphalt at high temperatures [40]. Fig. 9 presented the rutting factors of different types of asphalts at different temperatures. As the temperature increased, the rutting factor of the asphalt diminished. After adding carbon nanotubes or SBS modifiers into asphalt binder, the rutting factors were improved to different extents. As a filler to the SBS modified asphalt, carbon nanotubes had high rigidity so that they could provide a supporting for the structure of asphalt, thereby increasing the rutting factor of the asphalt, and effectively enhancing its high-temperature rutting resistance. The results of the temperature sweeping tests suggested that carbon nanotubes improved the high-temperature performance of SBS modified asphalt and enhanced the ability of asphalt binders to resist permanent deformation.

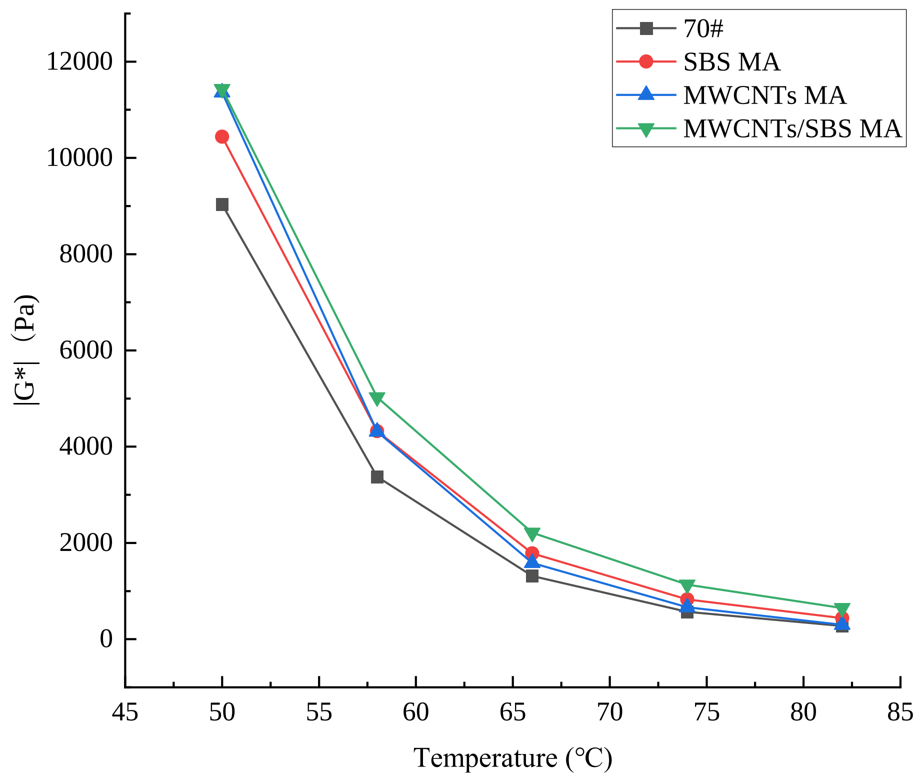

(a)

Preprints.org (www.preprints.org) | NOT PEER-REVIEWED | Posted: 24 April 2025 doi:10.20944/preprints202504.2078.v1

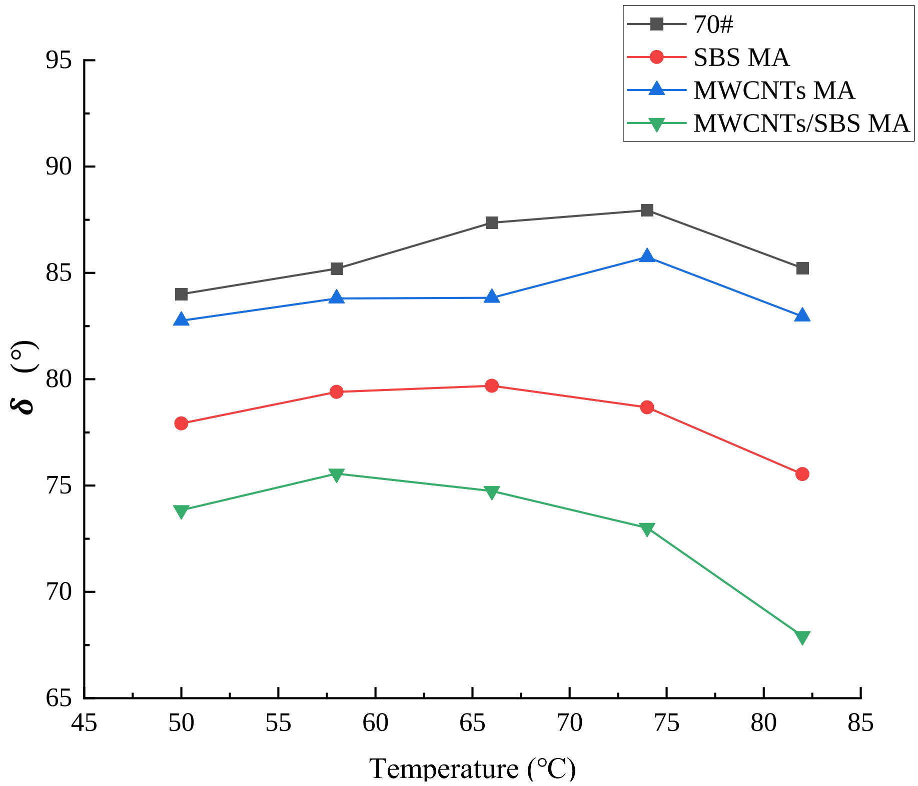

(b)

Figure 8. Temperature dependence of complex modulus and phase angle.

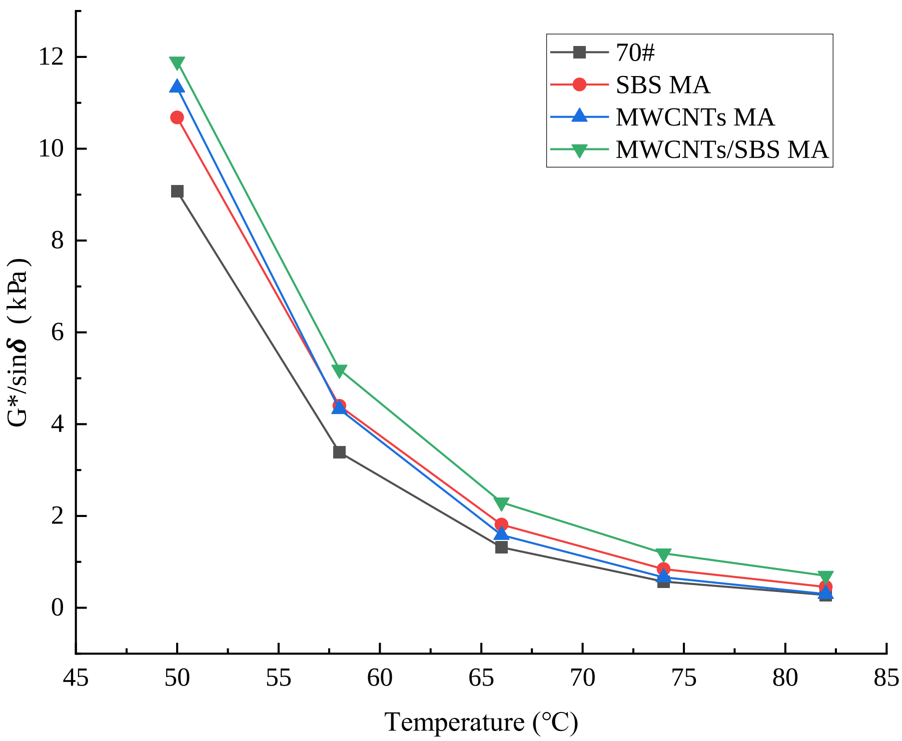

Figure 9. Rutting factor of different asphalts at different temperatures.

3.3. Multiple Stress Creep Recovery Test (MSCR)

3.3.1. Stress-Strain Characteristic Analysis

Preprints.org (www.preprints.org) | NOT PEER-REVIEWED | Posted: 24 April 2025 doi:10.20944/preprints202504.2078.v1

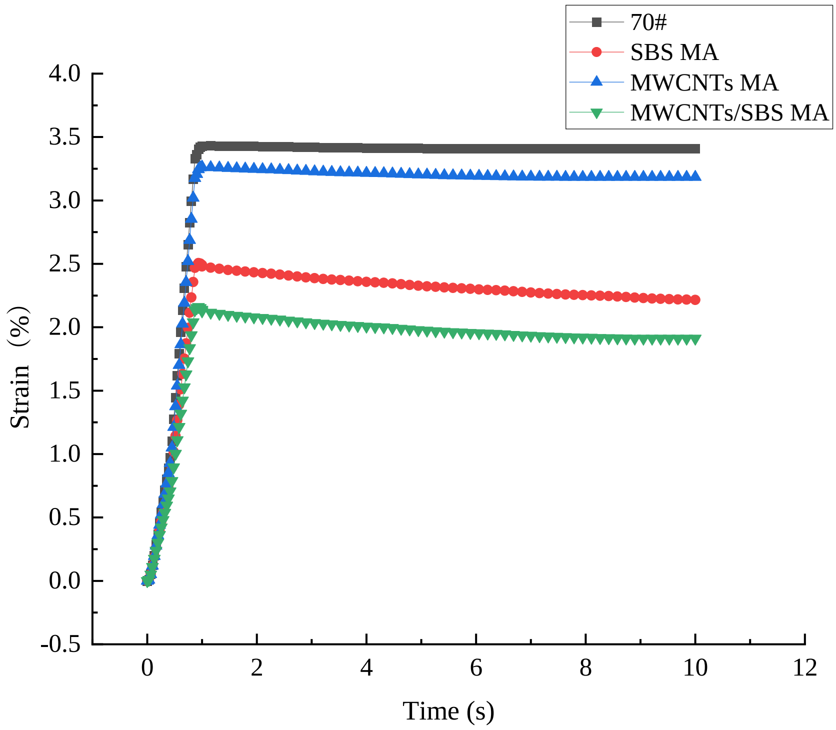

(a) **Shear strain under 0.1** kPa.

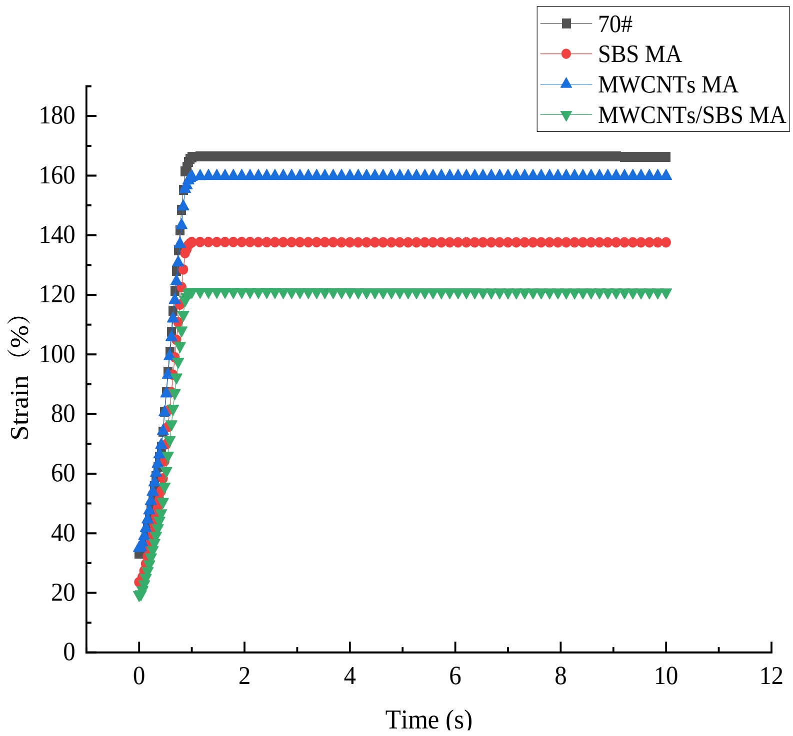

(b) **Shear strain under 3.2** kPa.

Figure 10. The curve of time-strain response under the first cycle.

Fig. 10 described the time-strain response in the first cycle at the temperature of 50℃. With the increase of the stress from 0.1 kPa to 3.2 kPa, the strain increased significantly, the strain-recovery became weaker, and the residual strain was larger, which means that the shear stress has a great impact on the recovery ability of asphalt. The strain of the base asphalt, SBS modified asphalt, carbon

Preprints.org (www.preprints.org) | NOT PEER-REVIEWED | Posted: 24 April 2025 doi:10.20944/preprints202504.2078.v1

nanotubes modified asphalt and MWCNTs/SBS composite modified asphalt at both stress levels of 0.1 kPa and 3.2 kPa were ranked as base asphalt＞carbon nanotubes modified asphalt＞SBS modified asphalt＞MWCNTs/SBS composite modified asphalt. In addition, the shear strain recovery rate of the MWCNTs/SBS composite modified asphalt was higher in comparison with the other three asphalts after the stress was unloaded, indicating that the addition of carbon nanotubes can effectively enhance the high-temperature deformation resistance of SBS modified asphalt.

3.3.2. Creep Characteristic Analysis

Present research has showed that the MSCR test can more effectively characterize the high-temperature performance of asphalt than the rutting factor. In this study, the unrecoverable creep compliance J_{nr} and creep recovery rate R of the base asphalt, SBS modified asphalt, carbon nanotubes modified asphalt and MWCNTs/SBS composite modified asphalt under different stress levels were measured through the multiple stress creep recovery test. The creep recovery rate R reflects the ability to return to its initial deformed state during the unloading stage. The non-recoverable compliance directly reflects the permanent deformation resistance of asphalt. The test results were shown in Fig. 11 and Fig. 12. It can be known that compared with the stress level of 0.1 kPa, $J_{nr3.2}$ is significantly higher than $J_{nr0.1}$, and $R_{3.2}$ is significantly lower than $R_{0.1}$. It verified that the higher the stress level, the more significant the influence on the deformation recovery of asphalt. The main reason was that the network restraining effect of carbon nanotubes and SBS was weakened attribute the increase in stress. As the temperature rises, the creep recovery rate decreases and the non-recoverable creep compliances shows an increasing trend, and the change trends were consistent for all samples. It can be explained that elastic component endows asphalt with an excellent capacity for deformation recovery. As the temperature rises, the fluidity of asphalt increases under high temperature, the enhancement of the viscous component increases the accumulation of unrecoverable deformation during the process of repeated loading and unloading. When evaluating the rutting resistance of asphalt binders under high-temperature conditions, the lower the J_{nr} value, the less the unrecoverable deformation, and the higher the R value, the more the recoverable elastic deformation. In this study, the three modified asphalts exhibited smaller J_{nr} values and larger R values compared with unmodified asphalt. This implied that adding MWCNTs/SBS modifier to the asphalt binder can effectively improve its rutting resistance at high temperature. The asphalt binder modified by MWCNTs+SBS modifier has the highest R value and the lowest Jnr value. It resulted from the fact that the carbon nanotubes were adsorbed on the surface of the SBS copolymer, which promoted the cross-linking between the SBS phase and the asphalt phase. The MSCR test showed that adding carbon nanotubes to the SBS modified asphalt can increase the elastic components of the asphalt binder so that the MWCNTs/SBS composite modified asphalt has excellent resistance to permanent deformation under high-temperature conditions.

Preprints.org (www.preprints.org) | NOT PEER-REVIEWED | Posted: 24 April 2025 doi:10.20944/preprints202504.2078.v1

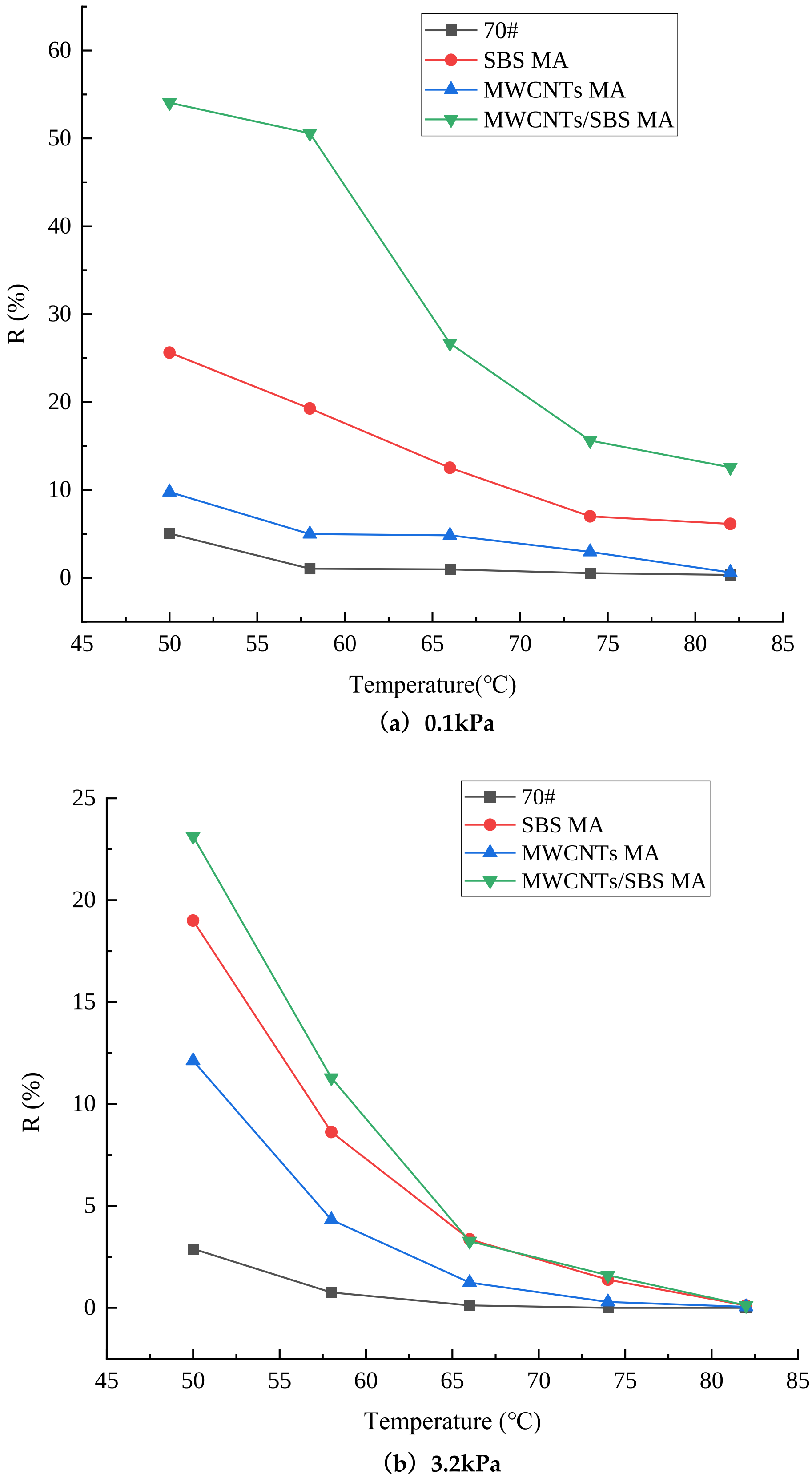

Figure 11. Creep recovery rate under different stress levels.

 doi:10.20944/preprints202504.2078.v1

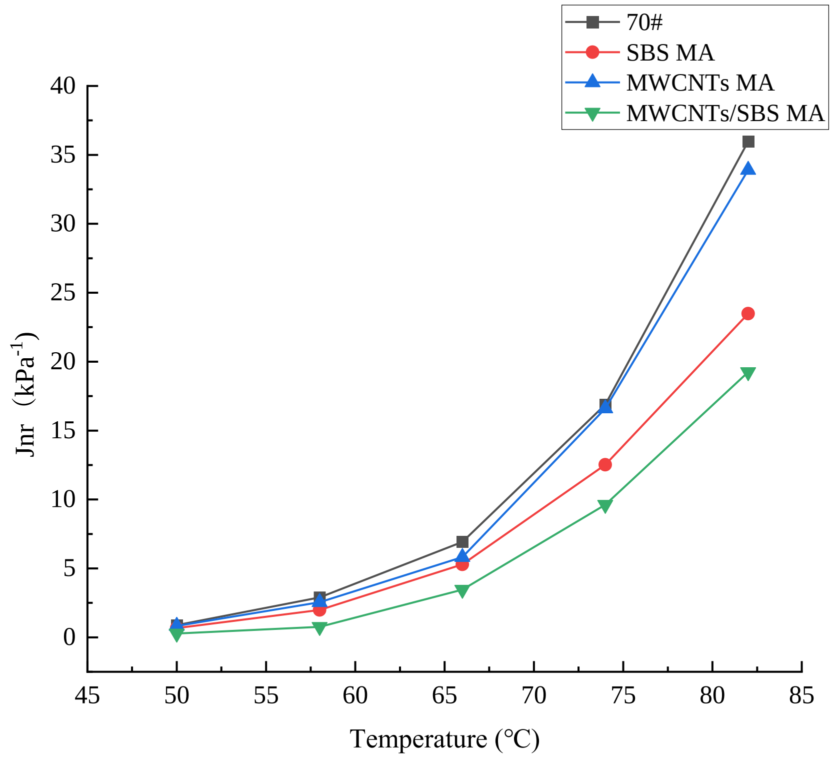

(a) **0.1kPa**

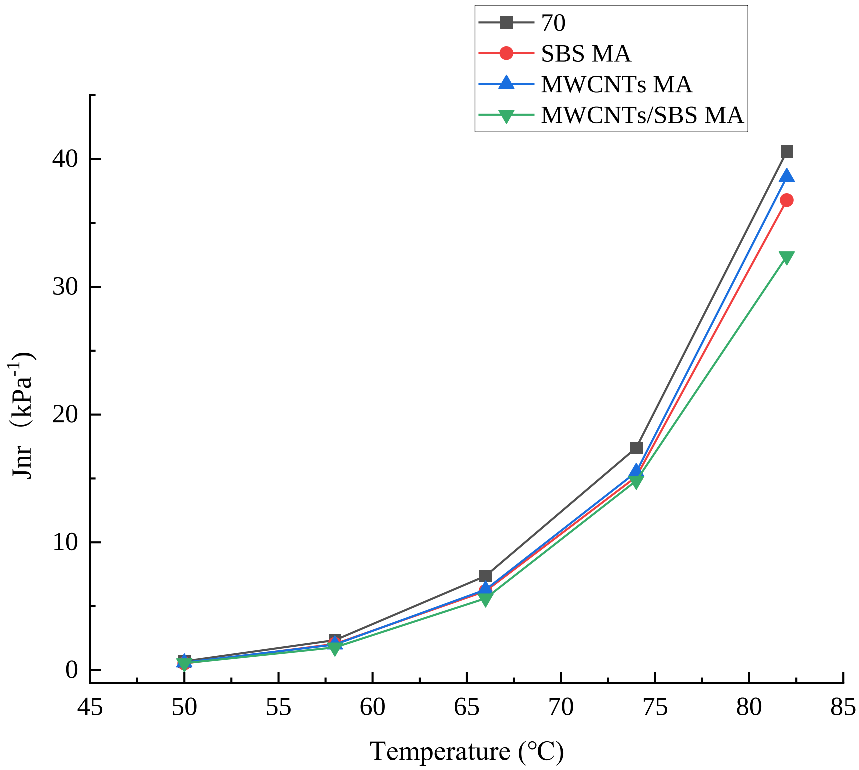

(b) **3.2kPa**

Figure 12. J_{nr} of different modified asphalts under different stress levels.

3.4. Micro-Properties

3.4.1. XRD Characterization

Fig. 13 and Table 8 described the XRD diffraction peak data and diffraction patterns of base asphalt, SBS modified asphalt, carbon nanotube modified asphalt and MWCNTs/SBS composite modified asphalt, respectively. As can be seen from Fig. 13, base asphalt, SBS modified asphalt, carbon nanotube modified asphalt and MWCNTs/SBS composite modified asphalt all exhibited obvious characteristic peaks at around 25° and 44°, corresponding to the (002) and (100) crystal planes, respectively. The intensity of the γ peak is too weak to be shown in the XRD spectrum. Hence, the γ peak was manually added through Gaussian peak fitting. This study focused on the γ peak and the (002) graphite peak to evaluate the crystal structure and crystallinity of asphalt. The (002) peak in the XRD patterns of asphalt originated from the diffraction phenomenon of polycyclic aromatic hydrocarbons, and the γ peak originated from the diffraction phenomenon of saturated hydrocarbons in the asphalt components. As seen in Fig. 13, four types of asphalt exhibited similar peak patterns, revealing that they may contain the same crystalline phase components. A higher intensity value means better crystallinity. The XRD intensities of different asphalts were in the order of MWCNTs/SBS composite modified asphalt > base asphalt > carbon nanotubes modified asphalt > SBS modified asphalt. It was obvious that the addition of MWCNTs/ SBS decreased the intensity of asphalt binder. Asphalt with MWCNTs+SBS modifiers showed exceed intensity in comparison with SBS modified asphalt, contributing to a better crystallinity. From the "Area" data in Table 8, the peak area of the γ and (002) peaks of the base asphalt was 1571.23573 and 36.17641, respectively. Compared with SBS/MWCNTs modified asphalt, the peak area of the base asphalt was larger, which indicated that the addition of SBS/MWCNTs reduced the crystallinity of the crystalline phase components in the asphalt mixture. The peak area of the γ and (002) peaks of MWCNTs+SBS composite modified asphalt was 2089.34551 and 270.0296, respectively, which were higher than SBS modified asphalt. This suggested that carbon nanotubes endowed SBS modified asphalt with better crystallinity and a higher content of the crystalline phase, which is consistent with the results of the intensity analysis. In addition, the XRD patterns showed that the interlayer distance of the MWCNTs/SBS composite modified asphalt is smaller in comparison with SBS modified asphalt, indicating that the addition of carbon nanotubes made the crystal structure of SBS modified asphalt more compact and ordered and enhanced the intermolecular force, thus, the deformation resistance of SBS modified asphalt was improved.

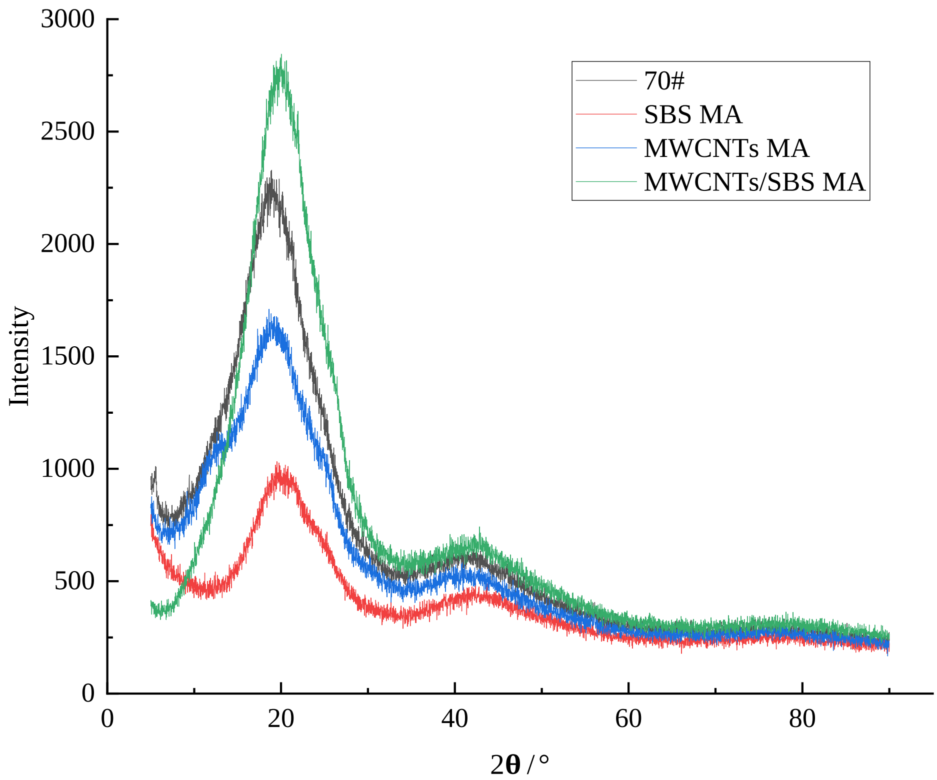

Figure 13. XRD patterns.

Table 8. Details of each diffraction peak.

Preprints.org (www.preprints.org) | NOT PEER-REVIEWED | Posted: 24 April 2025 doi:10.20944/preprints202504.2078.v1

Sample	peaks	2θ (°)	Peak height	FWHM	d (Å)	Area (mV·min)
Basic asphalt	γ-peak	18.90562	1571.23573	10.49541	5.84	17149.46669
	002-peak	25.53529	36.17641	1.62658	3.46	64.36886
SBS MA	γ-peak	20.18885	564.53763	8.67772	5.49	5199.52202
	002-peak	25.67987	50.56143	2.73259	3.44	147.07065
MWCNTs MA	γ-peak	18.64421	1094.23457	12.75621	5.91	14013.30848
	002-peak	25.12883	38.22032	1.17434	3.54	44.02699
MWCNTs/SBS MA	γ-peak	19.96733	2089.34551	8.47616	5.56	18797.32277
	002-peak	26.41321	270.0296	3.96452	3.36	1139.55181

3.4.2. Raman Characterization

This study mainly analyzed the characteristic peaks of the two modes (D peak and G peak) in the Raman spectrum to obtain their microscopic information. The D peak reflected the structural defects of MWCNTs. Such defects can promote the mutual fusion and interaction between MWCNTs and the components of the asphalt binder. Raman shift range was 1250-1450 cm^{-1}. The G peak reflected the tangential stretching vibration of the C=C bond in MWCNTs, and its Raman shift range was between 1500 cm^{-1} and 1605 cm^{-1}. The ratio of the intensity of the D peak to the G peak (I_D/I_G) characterized the degree of order of the system and the degree of interaction of each components, and its reciprocal (I_G/I_D) served as the graphitization index of MWCNTs [41]. The fitted Raman spectrum was shown in Fig. 14. The detailed information of the Raman spectrum peak were shown in Table 9. As can be seen from Fig. 14, D peak and G peak can be observed both in the Raman spectra of the base asphalt, SBS modified asphalt, carbon nanotube modified asphalt, and MWCNTs/SBS composite modified asphalt. There is no obvious shift in the Raman spectra of the D and G peaks. With the addition of MWCNTs, the intensity of the D peak of the SBS modified asphalt increased, and its structural defects increased. Adding MWCNTs/SBS into asphalt binders significantly increased the intensity of the G peak of in comparison with unmodified asphalt. Also, the intensity was increased from 6982.6528 for SBS modified asphalt to 8954.3102 when the SBS modified asphalt was modified by MWCNTs. The reason may be that the molecules of the asphalt components adhered to the MWCNTs, or the MWCNTs molecules penetrated into the SBS molecules, and the C=C bonds of different molecules interfered with each other. The I_D/I_G values of the base asphalt, SBS modified asphalt, carbon nanotube modified asphalt and MWCNTs/SBS composite modified asphalt were 0.9237, 0.4992, 0.8416 and 0.6137, respectively. After adding the MWCNTs/SBS modifier, the I_D/I_G value of the asphalt binder decreased to different extents. After adding MWCNTs to the SBS modified asphalt, the I_D/I_G value was decreased. The reason could be that during the composite-modification process, SBS and carbon nanotubes interacted with each other. SBS mainly reduced the relative intensity of the disordered carbon structure, and carbon nanotubes also have a certain effect. SBS and carbon nanotubes jointly optimized the order of the internal carbon structure of asphalt. It demonstrated that SBS with MWCNTs could reduce the defects of the SBS modified asphalt and improve its crystal quality.

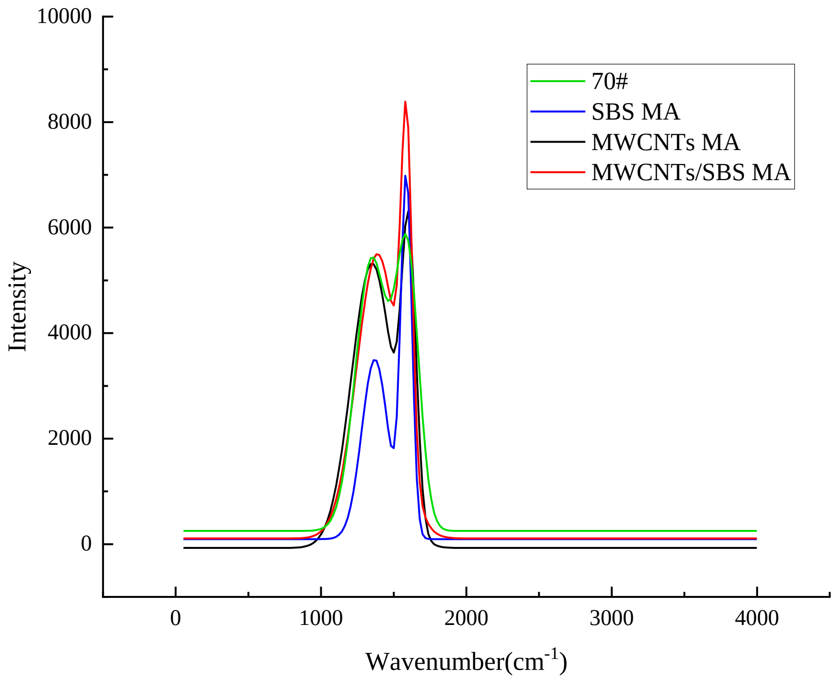

Figure 14. The fitting results of D peak and G peak.

Table 9. The Raman peak date of D peak and G peak.

Sample	W_D(cm^{-1})	I_D	W_G(cm^{-1})	I_G	I_D/I_G
Basic asphalt	1361.70	5433.2756	1579.80	5882.2022	0.9237
SBS MA	1361.70	3486.2060	1579.80	6982.6528	0.4992
MWCNTs MA	1361.70	5308.6607	1599.63	6307.8409	0.8416
MWCNTs/SBS MA	1381.53	5495.0786	1579.80	8954.3102	0.6137

4. Conclusions

In this study, the high-temperature performances of base asphalt, SBS modified asphalt, carbon nanotube modified asphalt, and MWCNTs/SBS composite modified asphalt were comprehensively investigated. In summary, the MWCNTs/SBS composite modified asphalt shows marked superiority in improving the high-temperature performance of asphalt, providing an effective material option for enhancing the service performance of asphalt pavements**.** The following main conclusions were obtained:

(1) In terms of physical properties, The softening points of the three modified asphalts have been increased by 2.6°C, 0.9°C, and 3.9°C respectively in comparison with the base asphalt. Compared with the base asphalt, the ductility of composite modified asphalt has also been improved, increasing from 215.6mm to 262.8mm. The modified asphalts are significantly superior to the base asphalt, and the composite modified asphalt performs most prominently in high-temperature performance. Whether carbon nanotubes or SBS are added, the viscosity of asphalt can be increased. Compared with the SBS modified asphalt, the viscosity values of the composite modified asphalt at each temperature increase by 0.11 Pa·s, 0.15 Pa·s, 0.111 Pa·s, 0.153 Pa·s, and 0.186 Pa·s , indicating that adding carbon nanotubes to SBS modified asphalt can further increase its viscosity and enhance its high-temperature rutting resistance.

(2) In the dynamic shear rheological test, the composite modified asphalt has the largest complex modulus in the low-frequency region, with strong rutting resistance, and it has a smaller slope in the high-frequency region which displays outstanding temperature-sensitive. The temperature sweep test shows that the composite modified asphalt has the largest complex shear modulus and the smallest phase angle, with remarkable high-temperature deformation resistance.

Preprints.org (www.preprints.org) | NOT PEER-REVIEWED | Posted: 24 April 2025 doi:10.20944/preprints202504.2078.v1

(3) The multiple stress creep recovery test (MSCR) shows that the composite modified asphalt has a smaller peak strain, a higher creep recovery rate, and the lowest non-recoverable creep compliance, demonstrating excellent deformation resistance and rutting resistance abilities at high temperatures.

(4) In terms of microscopic tests, XRD analysis shows that different modifiers have a significant impact on the crystalline-phase composition, crystallinity, and crystal structure of asphalt; Raman tests indicate that SBS modification has no obvious effect on the vibration energy of the chemical bonds of the disordered structure that generates the D peak. The addition of carbon nanotubes makes the D peak of the composite modified asphalt shift to the right and increases its intensity, and the G peak intensity is the highest. The I_D/I_G value reflects the synergistic optimization result of SBS and carbon nanotubes on the order of the internal carbon structure of asphalt.

Acknowledgments: This work was supported by the Natural Science Foundation of Shandong Province of China (No.ZR2022QE216), and this support is gratefully acknowledged.

References

1. Zhang Z, Liu H, Ban X, Liu X, Guo Y, Sun J, et al. Thermosetting resin modified asphalt: a comprehensive review. J Traffic Transport Eng (English Edition) 2023;10(6):1001–36.
2. Dongzhao Jin, Kai Xin, et al. Performance of rubber modified asphalt mixture with tire-derived aggregate subgrade[J]. Construction and Building Materials, 2024, 449: 138261.
3. Hongru Yao, et al. "Improvement on the high-temperature performance and fuel resistance of SBS modified asphalt by hybridizing with polyamideresin." Construction and Building Materials 309 (2021): 124987.
4. Kakar M R, Mikhailenko P, Piao Z, et al. Analysis of waste polyethylene (PE) and its by-products in asphalt binder[J]. Construction and Building Materials, 2021, 280: 122492.
5. Mojabi S A, Kordani A A, Hajikarimi P, et al. Evaluating fracture performance of stone mastic asphalt with SBS and SEBS modifications[J]. Theoretical and Applied Fracture Mechanics, 2024, 134: 104703.
6. Ren S, Liang M, Fan W, et al. Investigating the effects of SBR on the properties of gilsonite modified asphalt[J]. Construction and Building Materials, 2018, 190: 1103-1116.
7. Loise V, Vuono D, Policicchio A, et al. The effect of multiwalled carbon nanotubes on the rheological behaviour of bitumen[J]. Colloids and Surfaces A: Physicochemical and Engineering Aspects, 2019, 566: 113-119.
8. Monteiro, Liniker, et al. "Investigation of self-healing properties of nanoclay-modified asphalt binder using two-piece healing test." Canadian Journal of Civil Engineering 50.2 (2022): 126-136.
9. Ghabchi R, Castro M P P. Effect of laboratory-produced cellulose nanofiber as an additive on performance of asphalt binders and mixes[J]. Construction and Building Materials, 2021, 286: 122922.
10. Mansourkhaki A, Aghasi A. Low-temperature fracture resistance of asphalt mixtures modified with carbon nanotubes[C]//Proceedings of the Institution of Civil Engineers-Transport. Thomas Telford Ltd, 2021, 174(2): 78-86.
11. Xue, Z. H., & Fan, X. H. "Study on the Performance and Modification Mechanism of Carbon Nanotube - Modified Asphalt". New Building Materials, 2021, 48(6): 5. DOI: 10.3969/j.issn.1001 - 702X.2021.06.023.
12. Santagata E, Baglieri O, Tsantilis L, et al. Rheological characterization of bituminous binders modified with carbon nanotubes[J]. Procedia-Social and Behavioral Sciences, 2012, 53: 546-555.
13. Amin I, El-Badawy S M, Breakah T, et al. Laboratory evaluation of asphalt binder modified with carbon nanotubes for Egyptian climate[J]. Construction and building materials, 2016, 121: 361-372.
14. M. Gong, J. Yang, H. Yao, M. Wang, X. Niu, J.E. Haddock, Investigating the performance, chemical, and microstructure properties of carbon nanotube-modified asphalt binder, Road Mater. Pavement 19 (7) (2018) 1499–1522.
15. Goli, A.; Ziari, H.; Amini, A. Influence of carbon nanotubes on performance properties and storage stability of SBS modified asphalt binders. J. Mater. Civ. Eng. 2017, 29,04017070.
16. Shah P M, Mir M S. Investigating the influence of carbon nanotube on the performance of asphalt binder[J]. Progress in Rubber, Plastics and Recycling Technology, 2021, 37(4): 422-440.

Preprints.org (www.preprints.org) | NOT PEER-REVIEWED | Posted: 24 April 2025 doi:10.20944/preprints202504.2078.v1

17. Latifi H, Hayati P. Evaluating the effects of the wet and simple processes for including carbon Nanotube modifier in hot mix asphalt[J]. Construction and Building Materials, 2018,164:326-336.
18. Mamun A A, Arifuzzaman M.Nano-scale moisture damage evaluation of carbon nanotube-modified asphalt[J].Construction and Building Materials,2018,193:268-275.
19. Zhu, Y. Q., & Shu, B. A. "Influence of Carbon Nanotubes on the High and Low Temperature Performance of SBS - Modified Asphalt". Journal of Wuhan University of Technology (Transportation Science & Engineering), 2018, 42(1): 103 - 107.
20. Fu, Z., Tang, Y. J., Sun, Q. Y., et al. "Study on the Pavement Performance and Compatibility of Carbon Nanotube/SBS Composite - Modified Asphalt". Applied Chemical Industry, 2021, 50(8): 2031 - 2036.
21. Sun, Q. Y. "Study on the Rheological Properties of Carbon Nanotube/SBS Composite - Modified Asphalt". Dissertation, Chang'an University, 2020.
22. Obukhova S, Korolev E, Gladkikh V. The Influence of Single-Walled Carbon Nanotubes on the Aging Performance of Polymer-Modified Binders[J]. Materials, 2023, 16(24): 7534.
23. Tang Y, Fu Z, Ma F, et al. Carbon nanotubes for improving rheological and chemical properties of styrene–butadiene–styrene modified asphalt binder[J]. International Journal of Pavement Engineering, 2023, 24(1): 2211212.
24. Chen J, Huang Z, Wang H, et al. Investigating the rheological properties of styrene-butadiene-styrene-based high-viscosity modified asphalt using carbon nanotubes[J]. Sustainability, 2022, 15(1): 71.
25. Wang R , Yue M , Xiong Y ,et al. Experimental study on mechanism, aging, rheology and fatigue performance of carbon nanomaterial/SBS-modified asphalt binders[J].Construction and Building Materials, 2020, 268.DOI:10.1016/j.conbuildmat.2020.121189.
26. Yu C, Hu K, Chen G, et al. Molecular dynamics simulation and microscopic observation of compatibility and interphase of composited polymer modified asphalt with carbon nanotubes[J]. Journal of Zhejiang University-SCIENCE A, 2021, 22(7): 528-546.
27. Zhang X, Zhou X, Ji W, et al. Characterizing the mechanical properties of Multi-Layered CNTs reinforced SBS modified Asphalt-Binder[J]. Construction and Building Materials, 2021, 296: 123658.
28. Wang P, Zhai F, Dong Z, et al. Micromorphology of asphalt modified by polymer and carbon nanotubes through molecular dynamics simulation and experiments: Role of strengthened interfacial interactions[J]. Energy & Fuels, 2018, 32(2): 1179-1187.
29. Shu B, Wu S, Pang L, et al. The utilization of multiple-walled carbon nanotubes in polymer modified bitumen[J]. Materials, 2017, 10(4): 416.
30. Nie G, Huang W, Wu K, et al. Modification Mechanism of MWCNTs and SBS Composite modified Asphalt Binder: Laboratory Investigation and Molecular Dynamic Simulation[J]. Journal of Materials in Civil Engineering, 2024, 36(9): 04024279.
31. Xie Shuangrui. Experimental Study on the Influence of Carbon Nanotubes on the Performance of SBS Modified Asphalt and Mixtures[D]. Heilongjiang: Northeast Forestry University, 2020.
32. Yang Zhaohui. Research on Rheological Properties and Modifier Dosage of SBS Modified Asphalt[D]. Changan University, 2011. DOI: 10.7666/d.y1947258.
33. Zhu Haoran, Wei Jianming, Gong Minghui, et al. Research Progress of Carbon Nanotube Modified Asphalt[J]. Acta Petrolei Sinica (Petroleum Processing Section), 2017, 33(2): 386 - 394.
34. Ministry of Transport of the People's Republic of China. Test Specifications for Asphalt and Asphalt Mixtures in Highway Engineering (JTG E20 - 2011)[M]. China Communications Press, 2011.
35. Li Fujin, Shen Jinan. Implementation Manual of Technical Specifications for Construction of Highway Asphalt Pavement[M]. Beijing: China Communications Press, 2005.
36. ASTM. Standard viscosity-temperature chart for asphalt: ASTM D2493/2493M[S].USA:US-ASTM,2009.
37. Shen Jin'an. Road Performance of Asphalt and Asphalt Mixtures[M]. Beijing: China Communications Press, 2001.
38. Huang Wei, Guo Rongxin, Zhou Bin, et al. Research on Viscoelastic Behavior of SBS/PPA Modified Asphalt Based on Frequency Sweep[J]. Journal of Highway and Transportation Research and Development (Applied Technology Edition), 2016, 12(06): 134 - 136.

 doi:10.20944/preprints202504.2078.v1

39. M. L. Williams, R. F. Landel, J. D. Ferry. The Temperature Dependence of Relaxation Mechanisms in Amorphous Polymers and Other Glass-Forming Liquid [J]. Journal of American Chemical Society, 1955, 77(14): 3701–3707
40. Rusbintardjo G, Hainin M R, Yusoff N I M. Fundamental and rheological properties of oil palm fruit ash modified bitumen [J]. Construction and Building Materials, 2013, 49: 702-11.
41. Konstantinos, S, Andrikopoulos, et al. Evaluation of multi-walled carbon nanotube concentrations in polymer nanocomposites by Raman spectroscopy[J].Carbon: An International Journal Sponsored by the American Carbon Society, 2014, 76:301-309.